Journal of Materials Chemistry C

Accepted Manuscript

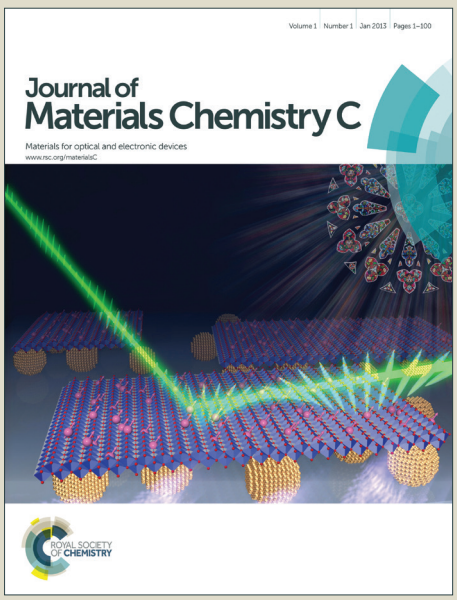

ROYAL SOCIETY OF CHEMISTRY

www.rsc.org/materialsC

Journal Name

RSCPublishing

ARTICLE

High ON/OFF Ratio Single Crystal Transistors based on Ultrathin Thienoacene Microplates

Cite this: DOI: 10.1039/xoxxoooooox

Xiaoli Zhao,[a] Tengfei Pei,[a] Bin Cai,[a] Shujun Zhou,[a] Qinxin Tang,*[a] Yanhong Tong,*[a] Hongkun Tian,*[b] Yanhou Geng[b] and Yichun Liu[a]

Received ooth January 2012,
Accepted ooth January 2012

DOI: 10.1039/xoxxoooooox

www.rsc.org/

The high ON/OFF ratio of organic single crystal field-effect transistors (FETs) are obtained based on dinaphtho[3,4-d:3′,4′-d′]benzo[1,2-b:4,5-b′]dithiophene (Ph5T2) ultrathin microplates. The ON/OFF ratio is over 10^8 with a small sweep range of gate voltage (<45 V) in air at room temperature when the dielectric is modified with octadecyltrichlorosilane (OTS). The high ON/OFF ratio is related to the decreased off-state current by molecular design and the increased on-state current by dielectric modification. The ON/OFF ratio up to1.3×10^7 can also be realized on a flexible transparent substrate. The ultrathin Ph5T2 single crystal provides the stable performance even though the flexible device experiences a bending/recovering test for 200 times. The high ON/OFF ratio combined with the high mobility up to 0.51 $cm^2V^{-1}s^{-1}$ as well as the good flexibility of the ultrathin organic single crystals shows their promising potential in electronic applications.

Introduction

Field-effect mobility and ON/OFF ratio are the two most important parameters to evaluate the performance of organic field-effect transistors (FETs).[1] The former indicates the ability of carrier migration and determines the switch velocity of devices and circuits. The latter indicates the capacity of resisting disturbance of devices and circuits.[2] Currently, most studies have focused on the optimization of the mobility.[3] The improvement of the ON/OFF ratio is generally neglected. However, in some practical applications, for example, in memory and logic circuits, a high ON/OFF ratio is even more important than a high mobility.[4] Currently, it is a challenge to obtain the high ON/OFF ratio in organic single crystal devices. The highly ordered structure and the absence of grain boundary defects in organic single crystals are favorable for high mobility, while dramatically improve the off-state current and hence lower the ON/OFF ratio (supporting information).[5]

Most organic single crystal FETs show the ON/OFF ratio in the order of 10^3-10^6 (a detailed performance list for the reported organic single crystal FETs is shown in Table S1 of supporting information). Only a few organic single crystal FETs with the ON/OFF ratio over 10^8 have been reported.[6] For example, Zhenan Bao's group has reported that the ON/OFF ratio of tetracene single crystal FETs was 10^5-10^8 with a sweep range of gate voltage from -100 to 10 V.[6a] They have also fabricated a lamination-type dinaphtho[2,3-b:2′,3′-f]thieno[3,2-b]-thiophene (DNTT) single crystal FET, with the ON/OFF ratio of 10^8 , by using Cytop-treated SiO_2 as gate dielectric and top-contact gold/tetrathiafulvalene-tetracyanoquinodimethane as electrodes.[6d] C. Daniel Frisbie's group has obtained tetracene single crystal FETs with ON/OFF ratios in excess of 10^9 when the test temperature was lowered down to 4.2 K.[6b] Oana D. Jurchescu's group has reported that 2,8-difluoro-5,11-bis(triethylsilylethynyl) anthradithiophene (diF-TESADT) single crystal FETs exhibited the ON/OFF ratios of 10^8 in N_2 with a small sweep range of gate voltage (~60 V).[6c] It is desirable that the organic single crystal FETs possess both the high mobility and the high ON/OFF ratio with a small sweep voltage as well as good air stability for practical applications. Until now, however, only few reports have addressed the methods to improve the ON/OFF ratio of organic single crystals.

We notice that the reported new materials with the high ON/OFF ratios,[6c,6d] such as DNTT and diF-TESADT, possess the similar molecular structures which contain the thiophene rings and introduce less electron donating subunits.[7] Therefore, the low highest occupied molecular orbital (HOMO) energy level could be formed, which can lower the off-state current and probably facilitates the improvement of the ON/OFF ratio.[7] Herein, we designed a thienoacene-based molecule with a low HOMO energy level (-5.85 eV),[8] dinaphtho[3,4-d:3′,4′-d′]benzo[1,2-b:4,5-b′]dithiophene (Ph5T2) (the molecular structure is shown in the inset of Figure 1), and fabricated its single crystal FETs. Its thin film transistors have show the good stability in air and the high field-effect performance.[8] In our experiments, its ultrathin single crystal FETs show the high mobility up to 0.51 $cm^2V^{-1}s^{-1}$ on octadecyltrichlorosilane (OTS)-modified Si/SiO_2 substrate. More importantly, the ON/OFF ratio measured in air at room temperature is over 10^8 with a small sweep range of gate voltage (<45 V). The ON/OFF ratio is extremely high for organic single crystal FETs, and two orders higher than that of the most reported organic single crystals FETs (Table S1, supporting information). The comparable mobility and ON/OFF ratio of Ph5T2 single crystals to the commonly used hydrogenated amporphous silicon (a-Si:H) show the potential of the Ph5T2 single crystals in broad applications, for example, in active matrix liquid crystal displays (AMLCD).[9]

Results and Discussion

Single crystals of Ph5T2 were grown by a physical vapor transport technique. The different-size crystals were grown on Si substrates by controlling the substrate location. Figure 1 shows the optical images, X-ray diffraction (XRD) result and selected area electron diffraction

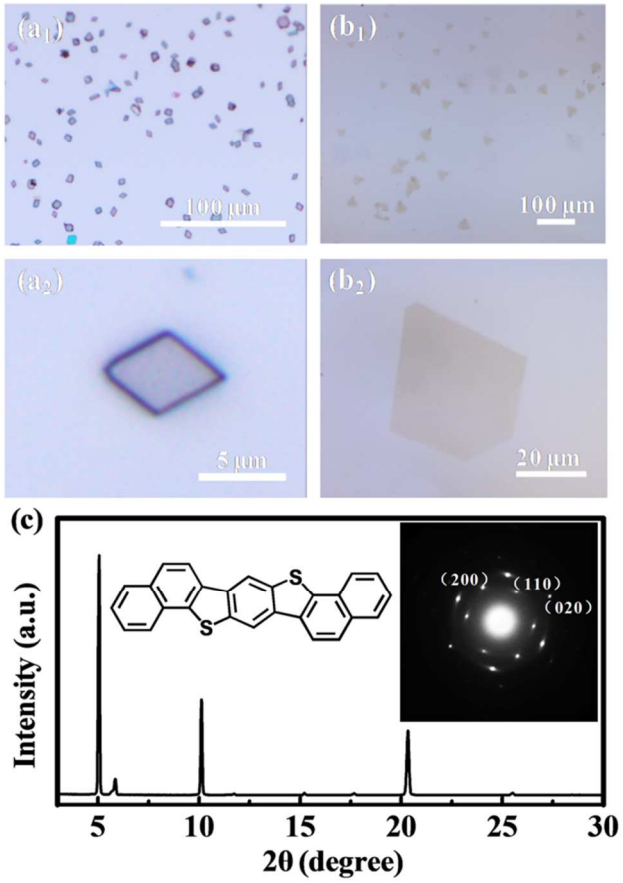

Figure 1. (a_1-b_2) Optical images of thick (a_1-a_2) and thin (b_1-b_2) Ph5T2 microplates. (c) XRD data of Ph5T2 microplates. The insets are the molecular structure of Ph5T2 and the SAED pattern of a typical microplate.

(SAED) pattern of the sample. The scanning electron microscopy (SEM) and atomic force microscope (AFM) images are shown in Figure 2. A large number of the dense thick microplates (Figure 1a_1 and 1a_2) were obtained when the substrate was put at the front end of the deposition zone. Some sparse thin microplates (Figure 1b_1 and 1b_2) were obtained at the back end of the deposition zone. The optical, SEM and AFM images (Figure 1a_1-b_2, Figure 2) show a great number of microplates well adhere on the substrate surface. These microplates show the regular rhombic shapes and the uniform colors, suggesting that these microplates may be crystals. The XRD result of the microplates is shown in Figure 1c. Three strong and sharp diffraction peaks at $2\theta = 5.06^o$, 10.12^o and 20.32^o are observed, corresponding to the primary, second-, and fourth-order diffraction in the [001] direction (i.e., *c* axis), respectively.[8] This multiple-angle relationship with the preferred orientation shows that the growth direction perpendicular to the substrate of these Ph5T2 microplates is [001].[10] It is in good agreement with the optical and SEM results. These Ph5T2 crystals exhibit layer-to-layer packing on the substrate. The *d*-spacing of 1.745 nm, which is calculated from the primary peak, is very close to the length of the Ph5T2 molecule (1.805 nm).[8] This suggests that Ph5T2 molecules are nearly perpendicular to the

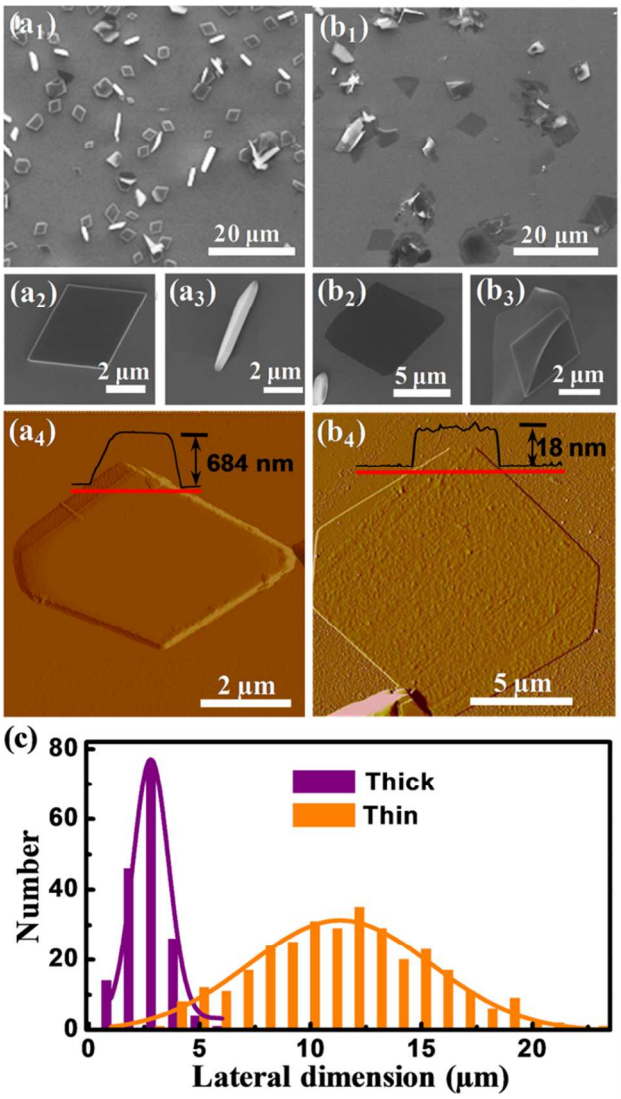

Figure 2. (a_1-a_4) Typical SEM and AFM images of thick Ph5T2 microplates. Figure a_3 shows the sectional view of a thick microplate. (b_1-b_4) Typical SEM and AFM images of thin Ph5T2 microplates. Figure b_3 shows the microplate is thin so that it bends and stands on the substrate. (c) The lateral dimension distribution of the thick and thin microplates obtained from optical images. The curves are the Gaussian fitting results.

substrate.[10a] The SAED pattern of the Ph5T2 microplate is shown in the inset of Figure 1c. A set of regular and clear diffraction spots confirm the nature of single crystals of these microplates. The length of crystal axis of Ph5T2 single crystals may be a^*=0.43 nm and b^*=0.30 nm, respectively. Two types of microplates with different colors were mainly observed on the Si substrate under the optical microscope. It is noticed that the color of the single crystals depends on their thickness which can be confirmed by combining the optical images and AFM results (Figure 1 and 2). The thick Ph5T2 single crystals are light gray (Figure 1a_1 and 1a_2), and the thin Ph5T2 single crystals present the color of earthy yellow (Figure 1b_1 and 1b_2). The AFM results show that the thickness of the light gray microplates ranges from 0.5-1.5 μm (Figure 2a_4), and the earthy yellow microplates have the thickness in 14-60 nm (Figure 2b_4). The molecular length of Ph5T2 is 1.805 nm, which suggests that the earthy yellow microplates consist of only a few to tens of molecule layers. According to the color difference of the microplates under the

optical images, the lateral size distribution of the thick (light gray) and the thin (earthy yellow) single crystals is shown in the histograms of Figure 2c. The statistical data of the lateral size distribution agrees well with the Gaussian fit presented by the purple and orange curves, respectively. The lateral sizes of all the thick microplates (light gray) are less than 5 μm, while the thin microplates (earthy yellow) have the larger lateral size ranging from several micrometers to tens of micrometers.

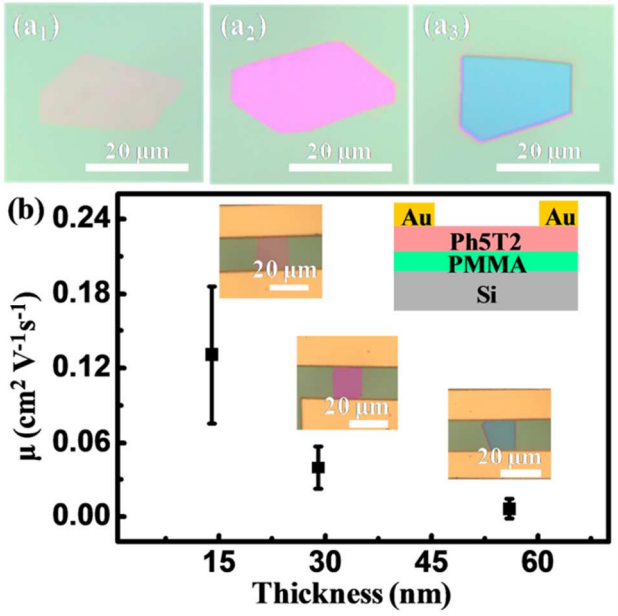

Figure 3. (a_1-a_3) Optical images of the ultrathin Ph5T2 single crystal microplates with the thicknesses of 14, 28 and 56 nm, respectively. (b) Thickness dependence of the mobility of the Ph5T2 single crystal FETs. The error bars indicate the standard error of the mean, obtained from statistical data for three kinds of single crystals with different colors. The insets are the schematic image of the device and the optical images of the devices with different crystal colors.

The SEM image in Figure $2b_3$ shows a thin crystal microplate standing on the substrate. The bent morphology suggests the good flexibility of the thin microplates. It combines the large lateral size make these thin crystal microplates possibly manipulated with the mechanical probe to realize the device fabrication. The smooth surface of the ultrathin crystals, as shown in AFM image of Figure $2b_4$, ensures the intimate contact between the crystal and the dielectric, which is one key to determine the performance of FETs.[11,6a] These thin Ph5T2 single crystals not only demonstrate their potential in flexible electronics,[12] but also meet the increasing demand for the miniaturization of organic electronics. Currently, most transistor devices apply the top-contact configuration. Compared with the bottom-contact, the top-contact configuration facilities enhancing the efficiency of carrier injection between semiconductor and electrodes for the higher mobility and at the same time remaining the high ON/OFF ratio.[13] It has been shown that the top-contact devices yield the mobilities that are typically higher by a factor of two compared with the bottom-contact devices.[13] However, for the top-contact devices, the source-drain current I_{SD} need cross the thickness of organic semiconductor for two times, which increases the parasitic resistance and limits the carrier injection and transport.[14] Therefore, these thin microplates may be favorable for the device fabrication with top-contact configuration.

Here, the thin Ph5T2 single crystals were transferred onto polymethyl methacrylate (PMMA) dielectric layer with the mechanical probe. The optical images in Figure $3a_1$-a_3 show that the color of the single crystals depends on their thickness. The single crystal is light pink when its thickness is ~14 nm, shifting to dark pink at ~28 nm, and finally blue at ~56 nm. Previous reports have also addressed the dependence of the material thickness on color. For example, K. S. Novoselov etc. have made a "color reference" to estimate the thickness of the graphene.[15] This provides us a facile way to estimate and select the single crystals with different thicknesses under the observation of the optical microscope for device fabrication. It is found that the Ph5T2 single crystal thinner than 60 nm are difficult to distinguish on SiO_2 substrate but can easily be seen on the PMMA surface possibly due to the added optical path that shifts the interference colors.[15] Therefore, PMMA is selected to study the relation of the color, thickness, and mobility of the Ph5T2 single crystal. Figure 3b shows the dependence of the mobility on the thickness of the Ph5T2 single crystal FETs on the Si/PMMA substrate. The Ph5T2 single crystal FETs with bottom-gate top-contact configurations were fabricated by the "gold film stamping" method.[16] The insets of Figure 3b are the schematic image of the device and the optical images of the devices with different crystal colors. The carrier mobility increases from 6.4×10^{-3} to 0.13 $cm^2V^{-1}s^{-1}$ with the decrease of the crystal thickness from 56 to 14 nm (Figure 3b), indicating the enhanced carrier injection for the thinner crystal. This confirms that the thinner single crystal is favorable for the improvement of the field-effect performance.

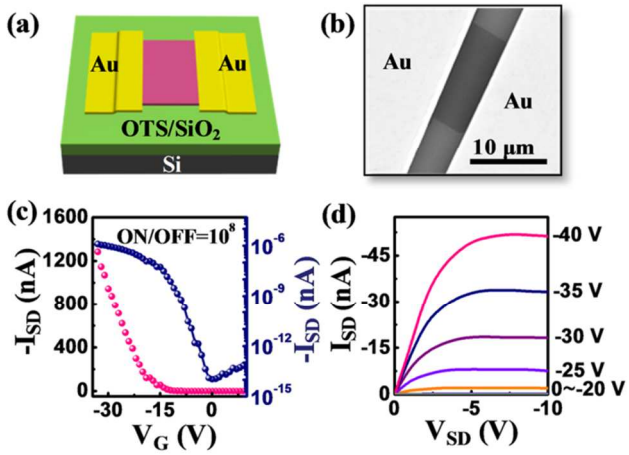

Figure 4. (a) Schematic image of the ultrathin Ph5T2 single crystal FET on OTS-modified Si/SiO_2 substrate. (b) SEM image of the FET device. The crystal is so thin that the contrast between the substrate and the crystal is low. (c, d) Typical transfer and output characteristics of the device measured at V_{SD}= -5 V in air at room temperature.

By optimization of the dielectric layers (PMMA, SiO_2 and OTS-modified SiO_2), Ph5T2 ultrathin (< 20 nm) single crystal FETs with the best performance was obtained on the OTS-modified Si/SiO_2 substrate. Figures 4a and 4b show the schematic and SEM images of the Ph5T2 single crystal FET on the OTS-modified Si/SiO_2 substrate. Figures 4c and 4d are the typical transfer and output characteristics of the ultrathin Ph5T2 single crystal FET. The Ph5T2 single crystal microplate consists of only a few to tens of molecule layers. All the fabricated transistors show the clear p-type characteristics with well-defined, linear and saturation regimes. The linear current-voltage characteristics at low source-drain bias (Figure. 4d) is consistent with a relatively low Schottky barrier to hole injection and thus low contact resistance,[3b] which possibly related to which possibly related to the ultrathin dimension of the crystal and the "gold film stamping" electrode fabrication technique (supporting information). The threshold voltage is ~-15 V. The field-effect mobility is as high as 0.51 $cm^2V^{-1}s^{-1}$. The device exhibits the ON/OFF current ratio of 10^8 with a small sweep range of gate

voltage from -35 to 10 V in air at room temperature. The ON/OFF ratio is extremely high for organic single crystals, and two orders of magnitude higher than that of the most reported organic single crystals (Table S1, supporting information). The small sweep range of gate voltage is favorable for reducing power dissipation and improving the ability of portability and security. Therefore, our Ph5T2 single crystal FETs with the high ON/OFF ratio under a small sweep voltage are promising for practical applications.

It has been addressed that it is difficult to obtain such a high ON/OFF ratio in single crystal devices and nanoscale devices.[5,17] The previously reported single crystal organic FETs with high ON/OFF ratio was generally obtained with a high sweep range of gate voltage, at an extremely low test temperature, or in a N_2 ambience (Table S1, supporting information). Even though only few reports have studied the factors that affect the ON/OFF ratio, increasing the sweep range of gate voltage is a general way to improve the ON/OFF ratio by increasing the on-state current.[18] In our Ph5T2 single crystal FETs, we believe that the high ON/OFF ratio could be ascribed to: i) the particular molecular structure, where the thiophene rings introduce less electron donating subunits.[7,19] In this case, the low HOMO energy level could be formed. The relatively low HOMO energy level can greatly reduce the carrier concentration at zero gate voltage.[7] In enhancement-mode FETs, the off current is determined by the carrier concentration present in device at zero gate voltage and the carrier mobility.[7] In our experiments, the threshold voltages of all the Ph5T2 single crystal devices are negative, indicating that the Ph5T2 single crystal FETs are enhancement-mode devices. Therefore, in our devices, the decreased carrier concentration at zero gate voltage by low HOMO energy level results in the low off-state current and hence the high ON/OFF ratio.[7] In general, the HOMO levels of the p-type organic semiconductors are in the range of 4.9-5.5eV.[20] The HOMO level of Ph5T2 is calculated to be -5.85 eV which is lower than that of most p-type organic semiconductors. Our experimental results show that the off-state current of the Ph5T2 devices is ~10^{-14} A. This value is lower than that of most p-type organic semiconductors, and is in good agreement with the theoretical predication based on HOMO level.[7] In addition, our experimental results show that all the Ph5T2 single crystal FETs with different dielectrics, for example, SiO_2, OTS-modified SiO_2 and PMMA, can obtain the ON/OFF ratio over 10^7. It confirms that the molecular structure can affect the ON/OFF ratio dramatically. In addition, another factor that affects the off-state current is the semiconductor thickness (Table S2 and Figure S2, supporting information). However, in our experiment, the off-state current of all the devices with the different crystal thickness is at the order of 10^{-14}. Therefore, the effect of the crystal thickness on the ON/OFF ratio is negligible. ii) Dielectric surface modification. In our experiments, the ON/OFF ratio of those devices with the OTS modification (10^8) is one order of magnitude higher than that of the devices without OTS modification (10^7, Figure S1). The transfer characteristics show that the off-state current of the Ph5T2 devices with and without OTS modification is almost equivalent (~10^{-14} A, Figure 4c and S1), while the on-state current of the device with OTS modification is about one order of magnitude higher than those without OTS modification. The OTS modification probably contributes to decrease the scattering states that disturb the carrier transport, i.e. decreases the carrier traps in the channel and hence improves the carrier transport and the ON/OFF ratio.[21] In our experiment, 10^{-14} A is the control limit of our equipment. Therefore, it can be predicted that the real ON/OFF ratio is possibly higher than 10^8.

In addition, the mobility of our devices with the OTS modification (0.51 $cm^2V^{-1}s^{-1}$) is higher than that of the device without OTS modification (0.15 $cm^2V^{-1}s^{-1}$, Figure S1), which is in good agreement with the previous reports. For example, Pernstich et al have reported that the pentacene FETs with OTS treatment exhibited the higher mobility and the smaller subthreshold swing than those FETs without OTS treatment.[21b] Recently, C. Effertz et al. have applied OTS monolayer with the different functional end-groups to demonstrate the effect of the adhesion energy of the dielectric on the field-effect mobility, and have given a quantitative evaluation of the correlation between adhesion energy and mobility.[22] In our experiments, the high mobility is believed to originate from the ultrathin dimension, the molecular structure of Ph5T2,[23] the nature of the single crystal[5] and the dielectric modification.[21] The high ON/OFF ratio combined with the high mobility shows the potential of Ph5T2 crystals as an alternative to the commonly used hydrogenated amporphous silicon (a-Si:H) in electronic applications, for example, in AMLCD, where the mobility greater than 0.5 $cm^2V^{-1}s^{-1}$ and the ON/OFF ratio greater than 10^8 are used.[9]

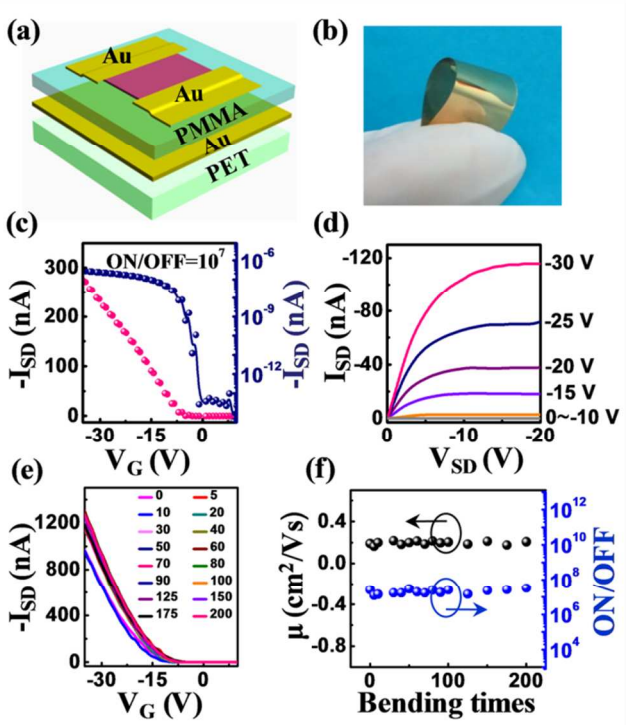

Figure 5. Flexible Ph5T2 ultrathin single crystal FETs. (a) Diagram of the basic design for transistor on plastic PET substrate with PMMA as dielectric. (b) Digital photo of flexible ultrathin single crystal transistors. (c, d) Output and transfer characteristics of a typical flexible device measured at V_{SD} = -5 V in air at room temperature. (e) The transfer curve of a flexible device before and after repeatedly bending. (f) The mobility and ON/OFF ratio variation before and after repeatedly bending at V_{SD} = -25 V.

Flexibility is an important characteristic and advantage for organic FETs.[12] Therefore, the flexible FETs was fabricated based on the ultrathin Ph5T2 single crystal. The schematic image of the flexible device is shown in Figure 5a. The flexible polyethylene terephthalate (PET) and PMMA is used as the supporting layer and the dielectric layer, respectively. Figure 5b is the digital photo of the Ph5T2 devices on the bending PET substrate. Figures 5c and 5d are the transfer and output curves of a typical device on the flexible PET substrate. The device has the high performance with the mobility as high as 0.435 $cm^2V^{-1}s^{-1}$ and the high ON/OFF ratio up to 1.3×10^7. The electrical characteristics of the flexible devices were multi-measured after the device was repeatedly bent to a radius of 2.5 mm

and then was recovered. The bending/recovering test was carried out for 200 times. Figure 5e shows the transfer curves of a typical flexible device before bending and after multiple bending cycles, from which the mobility and the ON/OFF ratio are extrapolated and their values before and after repeated bending are shown in Figure 5f. The mobility and ON/OFF ratio respectively are 0.197±0.016 $cm^2V^{-1}s^{-1}$ and (2.15±0.613) $\times10^7$. No significant loss in performance is observed after the process was repeatedly run for 200 cycles. This demonstrates that the ultrathin single crystal FET can endure strenuous bending, and therefore is a promising candidate for flexible electronics.

Conclusions

In summary, the ultrathin Ph5T2 single crystal microplates with thickness of a few to tens of molecule layers and length from 5 to 20 μm have been fabricated by the physical vapor transport technique. The transistors can be fabricated on the rigid substrate and the flexible transparent PET substrate. The carrier mobility increases with the decrease of the crystal thickness, indicating the advantage of the ultrathin crystal in the improved field-effect performance. Its ultrathin single crystal devices on the OTS-modified Si/SiO_2 substrate show the high mobility up to 0.51 $cm^2V^{-1}s^{-1}$, and the high ON/OFF ratio of over 10^8 with a small sweep range of gate voltage from -35 to 10 V in air at room temperature. The high ON/OFF ratio is related to the decreased off-state current by molecular design and the improved on-state current by OTS dielectric modification. Based on such ultrathin single crystals, the flexible Ph5T2 devices were fabricated and no significant loss in performance is observed after the device undergoes the repeated bending/recovering cycles for 200 times.

Experimental

Preparation of Ph5T2 single crystal and Instruments

Ph5T2 was synthesized as described previously.[8] Its single crystal microplates were fabricated by a physical vapor transport process in a horizontal tube furnace. At first the Ph5T2 powders were purified by sublimation in a high vacuum system. A quartz boat with the purified Ph5T2 powder was placed at the high-temperature zone and vaporized at 240 °C for 10 min. By controlling the temperature of source material and substrate location, different-size Ph5T2 microplates were grown on the Si, Si/SiO_2 and OTS-modified[24] Si/SiO_2 substrates. The high-purity nitrogen (99.999%) was used as the carrier gas, and the system was evacuated by a mechanical pump with chamber pressure at 25 Pa during the whole growth process. The optical images were obtained by Olympus microscope (BX51). The morphology of the microplates and the FETs were obtained using field-emission scanning electron microscopy (SEM; Micro FEI Philips XL-30 ESEM FEG). X-ray diffraction (XRD) measurements were carried out using a D/max 2500 XRD spectrometer (Rigaku) with Cu Kα line of 0.1541 nm. Selected-area electron diffraction (SAED) was carried out using a JEOL JEM-1011 transmission electron microscope (TEM) operated at an acceleration voltage of 100 kV. Atomic force microscopy (AFM) measurements were carried out on a SPA400HV instrument with a SPI 3800 controller (Seiko Instruments).

Device Fabrication and Measurement

FETs with bottom-gate top-contact configurations based on the microplates of Ph5T2 were fabricated by the "gold film stamping" method.[16] The high tenacity and good tractility of the Au made it feasible to stamp the thin Au layers onto the single crystal microplates as the source/drain electrodes.[11] Flexible Ph5T2 single crystal FETs were fabricated with PET as supporting layer and PMMA as dielectric. Au (50 nm) was evaporated on the 100 μm-thick PET sheets as gate electrode. PMMA was dissolved in anisole and deposited by spin coating on the Au film as the dielectric layer. The solvent of PMMA is anisole. PMMA was spin coated at 4000 rpm for approximately 40 s followed by thermal annealing at 100°C for 5 min. The thickness of PMMA insulation layer was ~300 nm. Dielectric capacitance is generally ~10 $nFcm^{-2}$. Current-voltage (I-V) characteristics of FETs were recorded with a Keithley 4200 SCS and a Cascade M150 probe station in a clean and shielded box at room temperature in air.

Acknowledgements

This work is supported by NSFC (51103018, 51273036, 61376074, 51272238, 512731926, 51322305, 61261130092), Ministry of Science and Technology of China (2012CB933703), 111 Project (B13013), 2009 National Excellent Doctoral Dissertation Award from China (201024), Program for New Century Excellent Talents of Ministry of Education (NCET-10-317), and Fundamental Research Funds for the Central Universities (11CXPY001, 12SSXM001).

Notes

[a] *Key Laboratory of UV Light Emitting Materials and Technology under Ministry of Education, Northeast Normal University, Changchun 130024, P. R. China. *E-mail: tangqx@nenu.edu.cn and tongyh@nenu.edu.cn*

[b] *State Key Laboratory of Polymer Physics and Chemistry, Changchun Institute of Applied Chemistry, Chinese Academy of Sciences, Changchun 130022, P. R. China. *E-mail: hktian@ciac.ac.cn*

† Electronic Supplementary Information (ESI) available. See DOI: 10.1039/b000000x/

References

1 G. Horowitz, *Adv. Mater.*, 1998, **10**, 365.

2 (a) G. H. Gelinck, H. E. A. Huitema, E. van Veenendaal, E. Cantatore, L. Schrijnemakers, J. B. P. H. van der Putten, T. C. T. Geuns, M. Beenhakkers, J. B. Giesbers, B.-H. Huisman, E. J. Meijer, E. M. Benito, F. J. Touwslager, A. W. Marsman, B. J. E. van Rens and D. M. de Leeuw, *Nature Mater.*, 2004, **3**, 106; (b) P. Andersson, R. Forchheimer, P. Tehrani and M. Berggren, *Adv. Funct. Mater.*, 2007, **17**, 3074; (c) S. Ju, J. Li, J. Liu, P.-C. Chen, Y. Ha, F. Ishikawa, H. Chang, C. Zhou, A. Facchetti, D. B. Janes and T. J. Marks, *Nano Lett.*, 2008, **8**, 997; (d) R. F. P. Martins, A. Ahnood, N. Correia, L. M. N. P. Pereira, R. Barros, P. M. C. B. Barquinha, R. Costa, I. M. M. Ferreira, A. Nathan and E. E. M. C. Fortunato, *Adv. Funct. Mater.*, 2013, **23**, 2153; (e) P. Gao, J. Zou, H. Li, K. Zhang and Q. Zhang, *Small*, 2013, **9**, 813.

3 (a) J. Chang, B. Sun, D. W. Breiby, M. M. Nielsen, T. I. Sölling, M. Giles, I. McCulloch and H. Sirringhaus, *Chem. Mater.*, 2004, **16**, 4772; (b) V. C. Sundar, J. Zaumseil, V. Podzorov, E. Menard, R. L. Willett, T. Someya, M. E. Gershenson and J. A. Rogers, *Science*, 2004, **303**, 16 Zhou, 44; (c) Y.T. Lei, L. Wang, J. Pei, Y. Cao and J. Wang, *Adv. Mater.*, 2010, **22**, 1484; (d) J. Smith, R. Hamilton, Y. Qi, A. Kahn, D. D. C. Bradley, M. Heeney, I. Mcculloch and T. D.

Anthopoulos, *Adv. Funct. Mater.*, 2010, **20**, 2330; (e) A. Lv, S. R. Puniredd, J. Zhang, Z. Li, H. Zhu, W. Jiang, H. Dong, Y. He, L. Jiang, Y. Li, W. Pisula, Q. Meng, W. Hu and Z. Wang, *Adv. Mater.*, 2012, **24**, 2626.

4 H. Sirringhaus, R. H. Friend, X. C. Li, S. C. Moratti, A. B. Holmes and N. Feeder, *Appl. Phys. Lett.*, 1997, **71**, 3871.

5 Q. X. Tang, H. Li, Y. Liu and W. Hu, *J. Am. Chem. Soc.*, 2006, **128**, 14634.

6 (a) C. R. Newman, R. J. Chesterfield, J. A. Merlo and C. D. Frisbie, *Appl. Phys. Lett.*, 2004, **85**, 422; (b) C. Reese, W.-J. Chung, M. -m. Ling, M. Roberts and Z. Bao, *Appl. Phys. Lett.*, 2006, **89**, 202108; (c) O. D. Jurchescu, S. Subramanian, R. J. Kline, S. D. Hudson, J. E. Anthony, T. N. Jackson and D. J. Gundlach, *Chem. Mater.*, 2008, **20**, 6733; (d) S. Haas, Y. Takahashi, K. Takimiya and T. Hasegawa, *Appl. Phys. Lett.*, 2009, **95**, 022111.

7 X. M. Hong, H. E. Katz, A. J. Lovinger, B.-C. Wang and K. Raghavachari, *Chem. Mater.*, 2001, **13**, 4686.

8 Y. Chen, H. Chang, H. Tian, C. Bao, W. Li, D. Yan, Y. Geng and F. Wang, *Org. Electron.*, 2012, **13**, 3268.

9 D. J. Gundlach, Y.-Y. Lin, T. N. Jackson, S. F. Nelson and D. G. Schlom, *IEEE Electron Device Lett.*, 1997, **18**, 87.

10 (a) J. Gao, R. Li, L. Li, Q. Meng, H. Jiang, H. Li and W. Hu, *Adv. Mater.*, 2007, **19**, 3008; (b) L. Jiang, W. Hu, Z. Wei, W. Xu and H. Meng, *Adv. Mater.*, 2009, **21**, 3649; (c) Z. Wei, W. Hong, H. Geng, C. Wang, Y. Liu, R. Li, W. Xu, Z. Shuai, W. Hu, Q. Wang and D. Zhu, *Adv. Mater.*, 2010, **22**, 2458.

11 Q. Tang, L. Jiang, Y. Tong, H. Li, Y. Liu, Z. Wang, W. Hu and Y. Liu, D. Zhu, *Adv. Mater.*, 2008, **20**, 2947.

12 (a) Y. Sun, H.-S. Kim, E. Menard, S. Kim, I. Adesida and J. A. Rogers, *Small*, 2006, **2**, 1330; (b) S. Kim, H. Y. Jeong, S. K. Kim, S.-Y. Choi and K. J. Lee, *Nano Lett.*, 2011, **11**, 5438; (c) W. J. Yu, S. Y. Lee, S. H. Chae, D. Perello, G. H. Han, M. Yun and Y. H. Lee, *Nano Lett.*, 2011, **11**, 1344; (d) F. Zhang, C. Di, N. Berdunov, Y. Hu, Y. Hu, X. Gao, Q. Meng, H. Sirringhaus and D. Zhu, *Adv. Mater.*, 2013, **25**, 1401; (e) D.-M. Sun, C. Liu, W.-C. Ren and H.-M. Cheng, *Small*, 2013, **9**, 1188.

13 (a) H. Sirringhaus, N. Tessler and R. H. Friend, *Science*, 1998, **280**, 1741; (b) Z. Bao, Y. Feng, A. Dodabalapur, V. R. Raju and A. J. Lovinger, *Chem. Mater.*, 1997, **9**, 1299.

14 Y. Zhang, H. Dong, Q. Tang, Y. He and W. Hu, *J. Mater. Chem.*, 2010, **20**, 7029.

15 K. S. Novoselov, A. K. Geim, S. V. Morozov, D. Jiang, Y. Zhang, S. V. Dubonos, I. V. Grigorieva and A. A. Firsov, *Science*, 2004, **306**, 666.

16 Q. X. Tang, Y. Tong, H. Li and W. Hu, *Appl. Phys. Lett.*, 2008, **92**, 083309.

17 Y. Cao, S. Liu, Q. Shen, K. Yan, P. Li, J. Xu, D. Yu, M. L. Steigerwald, C. Nuckolls, Z. Liu and X. Guo, *Adv. Funct. Mater.*, 2009, **19**, 2743.

18 (a) A. L. Briseno, R. J. Tseng, M. M. Ling, E. H. L. Falcao, Y. Yang, F. Wudl and Z. Bao, *Adv. Mater.*, 2006, **18**, 2320; (b) H. Jiang, H. Zhao, K. K. Zhang, X. Chen, C. Kloc and W. Hu, *Adv. Mater.*, 2011, **23**, 5075; (c) M. H. Hoang, D. H. Choi and S. J. Lee, *Synth. Met.*, 2012, **162**, 419; d) C. Mitsui, J. Soeda, K. Miwa, H. Tsuji, J. Takeya and E. Nakamura, *J. Am. Chem. Soc.*, 2012, **134**, 5448.

19 R. Li, L. Jiang, Q. Meng, J. Gao, H. Li, Q. Tang, M. He, W. Hu, Y. Liu and D. Zhu, *Adv. Mater.*, 2009, **21**, 4492.

20 R. Murphy and J. M. J. Fréchet, *Chem. Rev.*, 2007, **107**, 1066.

21 (a) D. Knipp, R. A. Street and A. Völkel, J. Ho, *J. Appl. Phys.*, 2003, **93**, 347; (b) K. P. Pernstich, S. Haas, D. Oberhoff, C. Goldmann, D. J. Gundlach and B. Batlogg, *J. Appl. Phys.*, 2004, **96**, 6431; (c) M. Kitamura and Y. Arakawa, *J. Phys.: Condens. Matter*, 2008, **20**, 184011; (d) S.-Z. Weng, W.-S. Hu, C.-H. Kuo, Y.-T. Tao, L.-J. Fan and Y.-W. Yang, *Appl. Phys. Lett.*, 2006, **89**, 172103.

22 C. Effertz, S. Lahme, P. Schulz, I. Segger, M. Wuttig, A. Classen and C. Bolm, *Adv. Funct. Mater.,* 2012, **22**, 415.

23 C. Wang, H. Dong, W. Hu, Y. Liu and D. Zhu, *Chem. Rev.*, 2012, **112**, 2208.

24 L. Wang, X. Zhang, Y. Fu, B. Li and Yi. Liu, *Langmuir*, 2009, **25**, 13619.

TOC

Based on Ph5T2 and the OTS modification of the dielectric, the ultrathin single crystal microplate transistors with the high ON/OFF ratio up to 10^8 can be obtained.